

# Understanding of the H-mode Pedestal Characteristics using the Multi-machine Pedestal Database

T. Hatae 1), M. Sugihara 2), A. Hubbard 3), Y. Igitkhanov 2), Y. Kamada 1),  
G. Janeschitz 2), L. Horton 4), N. Ohyabu 5), T. Osborne 6), M. Osipenko 7),  
W. Suttrop 4), H. Urano 8), H. Weisen 9)

- 1) Japan Atomic Energy Research Institute, Naka-machi, Ibaraki-ken, Japan
- 2) ITER Joint Central Team, Garching, Germany
- 3) MIT Plasma Science and Fusion Center, Cambridge, MA, USA
- 4) Max Planck Institut für Plasmaphysik, Garching, Germany
- 5) National Institute for Fusion Science, Gifu-ken, Japan
- 6) General Atomics, San Diego, USA
- 7) Kurchatov Institute, Moscow, Russia
- 8) Hokkaido University, Hokkaido, Japan
- 9) Centre de Recherches en Physique des Plasmas, Ecole Polytechnique Fédérale de Lausanne, Switzerland

e-mail contact of main author: hatae@naka.jaeri.go.jp

**Abstract.** With the use of a multi-machine pedestal database, essential issues for each regime of ELM types are investigated. They include (i) understanding and prediction of pedestal pressure during Type I-ELMs which is a reference operation mode of a future tokamak reactor, (ii) identification of the operation regime of Type-II ELMs which have small ELM amplitude with good confinement characteristics, (iii) identification of upper stability boundary of Type-III ELMs for access to the higher confinement regimes with Type-I or -II ELMs, (iv) relation between core confinement and pedestal temperature in conjunction with the confinement degradation in high density discharges. Scaling and model-based approaches for expressing pedestal pressure are shown to roughly scale the experimental data equally well and initial predictions for a future reactor case could be performed by them. It is identified that  $q$  and  $\delta$  are important parameters to obtain the Type-II ELM regime. A theoretical model of Type-III ELMs is shown to reproduce the upper stability boundary reasonably well. It is shown that there exists a critical pedestal temperature, below which the core confinement starts to degrade.

## 1. Introduction

The characteristics of the H-mode edge pedestal are crucial for characterizing the confinement and stability properties of the core plasma and for quantifying the effect of ELM energy load on divertor. Understanding and prediction of pedestal pressure during Type I-ELMs which is a reference operation mode of a future tokamak reactor are essential. Exploration of operation regimes which have small ELM amplitude with good confinement characteristics is also important. The operation regime of Type-III ELMs should be identified to access the higher confinement regimes with Type-I or -II ELMs. Analysis results on these issues using a multi-machine pedestal database archived from major divertor tokamaks, ASDEX-Upgrade (AUG), Alcator C-Mod (C-Mod), DIII-D, JET and JT-60U, are presented in this paper. Analysis of the relation of core confinement and pedestal and a possible method to obtain improved pedestal conditions in high density discharges are also presented.

## 2. Pedestal Pressure During the Type-I ELM Phase

To examine discharge parameter and machine size dependence of the pedestal pressure in the Type-I ELM phase, we employ the following two approaches; scaling approach and model based approach. In the first approach, the offset non-linear confinement scaling for ELM H-mode plasmas proposed in [1] is used. Experimental data are compared with the pedestal part of this scaling. In the second approach, the pedestal width model proposed in [2] is used together with the analytical expression for the critical pressure gradient determined by the

ideal ballooning mode assuming that the gradient in the Type-I ELMy phase is close to this stability boundary (first stability boundary).

From the offset non-linear confinement scaling, the total thermal stored energy  $W_{th}$  in an ELMy H-mode plasma is expressed as follows [1]

$$W_{th} = 0.082\kappa R a I_p B_t (B_t R^{1.25})^{-0.1} + 0.043 R^{1.3} a (I_p n_{19} P)^{-0.15} \quad (1)$$

The first term indicates the offset part determined by the MHD stability of the ELM. If we assume that the first term corresponds to the pedestal stored energy, the pedestal pressure  $p^{ped}$  can be expressed as follows.

$$p^{ped} = 2.8 \times 10^{-3} I_p B_t / a (B_t R^{1.25})^{-0.1} \quad (2)$$

Comparison of Eq. (2) with experimental  $p^{ped}$  is shown in Fig. 1(a). We found that AUG, DIII-D, JET and JT-60U data are roughly fitted by this scaling. C-MOD data are not included in this comparison, since regular Type-I ELMs have not been observed in C-MOD. It is interesting to note that the pedestal pressure is roughly expressed by some typical engineering parameters (i.e.  $I_p$ ,  $B_t$ ,  $a$  and  $R$ ) not including  $T_e$  and  $n_e$ . For discharges with fixed  $I_p$  and  $B_t$  in each machine, this scaling predicts the same pedestal pressure, though, in some machines, e.g., DIII-D, JET, the pedestal pressure varies with varying plasma density. Such data lie vertically in the figure, which implies that some other parameter dependence may be needed for further improvement of the scaling.

In the model-based approach, we employ the model for pedestal width  $\Delta_{ped}$  proposed in [2], which is expressed as  $\Delta_{ped} \propto \rho_{tor} S^2$  ( $S$ ,  $\rho_{tor}$  are magnetic shear and toroidal Larmor radius, respectively). Employing a simple analytic formula for the critical pressure gradient  $\nabla p_c^{ped}$ , the resultant expression for the pedestal pressure is written as follows.

$$p^{ped} = \nabla p_c^{ped} \Delta_{ped} \propto \frac{B_t^2}{R q^2} S \times \rho_{tor} S^2 \propto \frac{I_p \sqrt{T^{ped}}}{q a^2 (1 + \kappa^2)} S^3 \quad (3)$$

Magnetic shear in the pedestal region is significantly affected by bootstrap current driven by the steep pressure gradient. Although, in some machines, calculated the magnetic shear data by e.g., the EFIT code are archived, shear data derived from current profile measurement are not available in the present database. Thus, we will examine here the expression with magnetic shear effect omitted. Comparison of this expression with the experimental  $p^{ped}$  is shown in Fig. 1(b). It is seen that JET, AUG, and JT-60U data in the present database lie roughly on the diagonal line, though there are some separations between machines. Some deviation of DIII-D data from the diagonal line could be interpreted by their much steeper pressure gradient due to the second stability regime, which is out of scope of this model. Separation between each machine e.g., JET and JT-60U might be reduced by the inclusion of magnetic shear, which is to be confirmed by the archive of shear data in future. Inclusion of the magnetic shear effect has been partially examined in [2], and it has been demonstrated that the systematic deviation in JET data from the dependence of Eq. (3) without shear, can be improved by introducing the calculated shear. It has also been shown that the spatial profile of magnetic shear naturally introduces almost linear machine size dependence of the width, which distinguishes this model from simple Larmor radius scaling [2]. In concluding these studies, both approaches can roughly scale the experimental data equally well and initial prediction for a future reactor could be performed by them. However, further improvement in both approaches is needed, as indicated above.

### 3. H-mode regimes with small ELMs

While the Type-I ELM is the most common H-mode regime, it is recognized that, with high pedestal pressure, the energy loss associated with each ELM can be large. There is a serious

concern for reactor-scale devices that divertor erosion due to ELMs could be unacceptably high [3], motivating the search for regimes with good confinement but much smaller ELMs. Such regimes have been found on several experiments, including the ‘Low Particle Confinement’ (LPC) H-mode on JET [4], the Enhanced D<sub>α</sub>(EDA) H-mode on Alcator C-Mod [5], and Type II or grassy ELMs on DIII-D [6] and JT-60U [7]. While these differ in some details, they all have energy confinement  $\tau_E$  as good as, or even better than, Type-I ELMy H-mode and low particle confinement, preventing impurity buildup.

Type-II or ‘grassy’ ELMs have been frequently observed on both DIII-D and JT-60U. They appear to be periodic MHD events, similar to Type-I or -III ELMs but at much higher frequency and smaller amplitude. On JT-60U, the width and height of the  $T_i$  pedestal, and thus  $\tau_E$ , can increase above values with Type-I ELMs. In the C-Mod EDA regime, in contrast, periodic MHD relaxations are normally not observed. Enhanced particle transport is caused by continuous, quasi-coherent fluctuations which are localized in the density pedestal region. These have  $f \sim 100$  kHz in the lab frame and  $k_\theta \sim 3\text{-}6$  cm<sup>-1</sup>. EDA H modes have similar pedestals, and only slightly reduced  $\tau_E$ , compared to ELM-free H modes. The LPC H modes on JET [4] share many characteristics of the EDA regime.

Using the pedestal database, as well as published studies on each machine, the conditions for obtaining small ELMs on various experiments have been compared and many similarities found. Shaping is generally an important factor. On DIII-D, Type-II ELMs were observed only at high elongation,  $\kappa > 1.8$  and triangularity,  $\delta > 0.4$ .  $\delta_{av} > \sim 0.4$  was also required on both JT-60U [8] and C-Mod [9]. These experiments also find a lower limit for the safety factor  $q_{95}$  ( $> \sim 3.5$  on C-Mod,  $> \sim 4$  on JT-60U). Recently small ELMs, which may be Type II, have been reported on AUG with  $\delta_{av} > 0.4$  and  $q_{95} > 4.5$  [10]. The operational spaces for Grassy ELMs and EDA, on JT-60U and C-Mod respectively, are compared in Fig. 2. The similarity between them, and to conditions on AUG, suggests that, despite the differences in observed edge phenomena, there may be common physics in the regimes. Edge density fluctuations have not yet been measured in the JT-60U Grassy ELM regime, so it is not known if these play a role. JT-60U generally operates at higher  $\beta$  than C-Mod, which might explain the more apparent magnetic signatures. In fact, at  $\beta_N > 1.2$  some small ELMs have been seen in addition to the coherent fluctuations on C-Mod. Small ELM regimes have been observed on various machines with ohmic, ICRF and NB heating, showing that they are not related to heating method or fast particles.

#### 4. Regimes of Type III ELMs

The regime in which Type-III ELMs are found has been compared with a recent model [11,12]. This model presumes that the Type-III ELMs are driven by the interchange resistive instability caused by magnetic stochasticity (flutter), so-called RI-F instability. This mode is stabilized by electric field shear, which provides the upper boundary in the average pedestal temperature for Type-III ELMs. Comparison of this upper boundary with AUG and DIII-D are shown in Figs. 3 (a) and (b), respectively.

It is seen that the theoretical prediction can well reproduce the upper boundary for the Type-III ELM regime in both machines. Examinations on C-MOD also show good agreement with the theory. According to these comparisons, the theory could be a possible candidate for the Type-III ELMs, while more detailed comparison for wide parameter ranges will be necessary to improve the theory or to explore other possible models.

#### 5. Boundary condition for core confinement

In order to achieve sufficiently high fusion gain and high radiative power in the SOL and

divertor regions, high density operation is essential for a tokamak reactor. However, energy confinement (the H factor) in ELMy H modes tends to degrade with increasing density. This section introduces the database of pedestal parameters as the boundary condition for the core confinement and suggests a method to obtain improved pedestal conditions at a high density. It has been observed in the Type-I ELMy regime that the temperature at the pedestal shoulder decreases with an increase pedestal density (see Fig. 4(a)). Experimentally, there are two typical cases in the pedestal pressure when density or gas puffing rate is increased. In JT-60U and AUG, the pedestal pressure remains roughly constant ( $n^{ped} T^{ped} \sim \text{const.}$ ) for fixed  $I_p$ ,  $B_t$  and plasma shape [13-15]. In JET, the pedestal pressure gradually decreases with density [16]. The energy confinement during H modes depends in both cases strongly upon the pedestal temperature as shown in the Fig. 4(b) [17]. In this dataset, it can be seen that once a critical temperature is exceeded ( $T_e^{ped} \sim 1.3\text{-}1.4$  keV) the impact of the pedestal temperature on the energy confinement weakens. To determine whether the critical temperature is universal or would vary in other conditions, further study is necessary. A confinement improvement with increasing pedestal temperature takes place below the critical pedestal temperature. It should be noted here that confinement degradation at a high density is mainly attributed to the core confinement deterioration. Thus, in the H mode where the pedestal pressure is limited by Type-I ELMs, an increase in the pedestal density reduces the pedestal temperature, and if the pedestal temperature becomes lower than a certain level, confinement starts to degrade with decreasing temperature or increasing density. One observes an increase in the density where confinement degradation sets in with increasing triangularity because the pedestal pressure increases with triangularity (by  $\sim 40\%$  from  $\delta = 0.1$  to  $0.45$  in JT-60U). In a high density regime, the H factors are observed to increase with triangularity in JT-60U [18], AUG [19] and JET [16]. In high triangularity discharges, the pedestal temperature becomes higher and a higher energy confinement of the core plasma can be obtained at a given pedestal density.

## References:

- [1] TAKIZUKA T., Plasma Physics and Controlled Fusion **40**, 851 (1998).
- [2] SUGIHARA, M. "A Model for H-mode Pedestal Width Scaling Using the International Pedestal Database", to appear in Nucl. Fusion.
- [3] ITER Physics Expert Groups on Divertor, Divertor Modelling and Database and ITER Physics Basis Editors, Nucl. Fusion **39**(12), 2391 (1999).
- [4] BURENS, M, CAMPBELL, D.J., GOTTARDI, N., et al., Nucl. Fusion **32**, 539 (1992).
- [5] GREENWALD, M., et al., Physics of Plasmas **6**(5), 1943. (1999).
- [6] OZEKI, T., CHU, M.S., LAO, L.L., et al., Nucl. Fusion **30**, 1425 (1990).
- [7] KAMADA, Y., et al, Plasma Physics and Controlled Fusion **38**, 1387-1391 (1996).
- [8] KAMADA, Y., et al, Plasma Physics and Controlled Fusion **40**, A247-A253 (2000).
- [9] GREENWALD, M., et al., Plasma Physics and Controlled Fusion **40**, A265-A269 (2000).
- [10] STOBER, J., et al., Plasma Physics and Controlled Fusion **42**, A211-A216 (2000).
- [11] POGUTZE, O., et al., Proc. of the Edge Plasma Theory and Simulation Workshop, Innsbruck, Czech. J. Phys. **48/2** (1998).
- [12] IGITKHANOV, Yu., et al., "Physics of the L-H transition and Type III-ELMs phenomena (scaling properties and dimensionless analysis)", to appear in Contributions to Plasma Physics (7<sup>th</sup> PET Workshop, Toki, Japan, 1999).
- [13] ITER Physics Basis, Nucl. Fusion **39**, 2137 (1999).
- [14] URANO, H., et al., "Thermal Energy Confinement Properties of ELMy H-mode in JT-60U", submitted to Plasma Phys. Control. Fusion.
- [15] HORTON, L.D., Plasma Phys. Control. Fusion **41**, B329 (1999).
- [16] SAIBENE, G., et al., Nucl. Fusion **39**, 1133 (1999).
- [17] JANESCHITZ, G., et al., Proc. 26th the EPS Conf. on Control. Fusion and Plasma Phys., Maastricht (Geneva: EPS) vol. **23J**, 1445 (1999).
- [18] KAMADA, Y., et al., Proc. 16th Int. Conf. on Fusion Energy 1996, Montreal (Vienna: IAEA) vol. **1** 247 (1997).
- [19] STOBER, J., et al., Proc. 26th the EPS Conf. on Control. Fusion and Plasma Phys., Maastricht (Geneva: EPS) vol. **23J**, 1401 (1999).

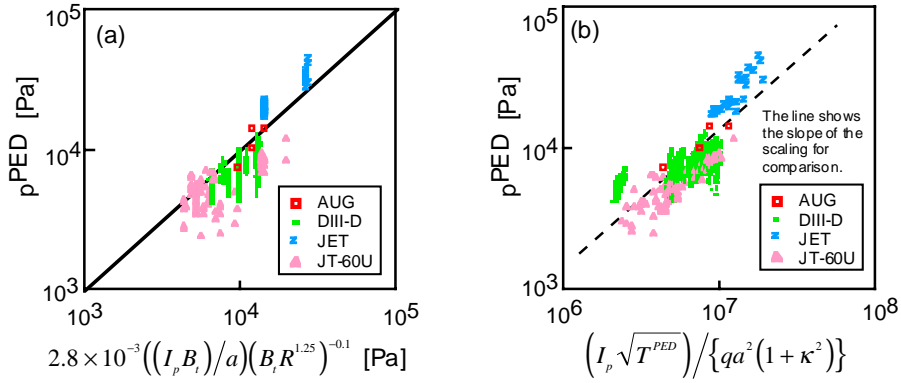


FIG. 1. The pedestal pressure is compared with (a) Offset non-linear scaling and (b) Sugihara's model [2].

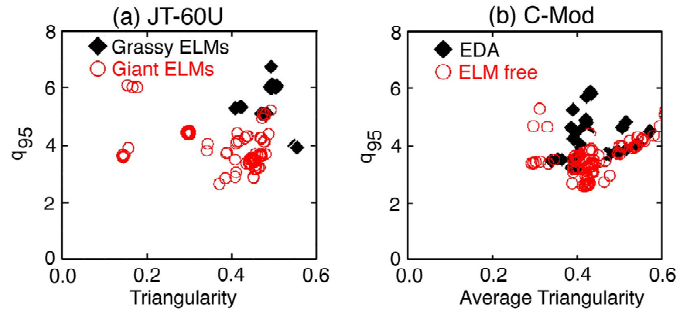


FIG. 2. The operational spaces for (a) Grassly ELMs on JT-60U and (b) EDA on C-Mod.

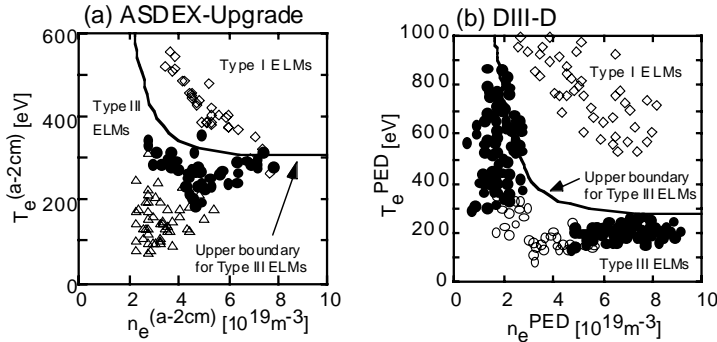


FIG. 3. Upper boundaries for the Type-III ELMs (upper curve) in AUG (a) and DIII-D (b). Diamonds and closed circles show Type-I ELMs and Type-III ELMs, respectively. Triangles and open circles show L-mode prior transition and early H-mode, respectively.

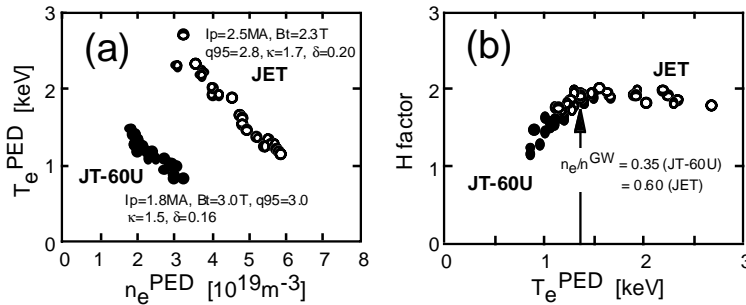


FIG. 4. (a) Edge operational space diagram for Type-I ELMy H-mode plasmas. Open and closed circles denote JET and JT-60U discharges, respectively. (b) Dependence of the H factor on the pedestal temperature in JET and JT-60U.